

**AMYLOID PRECURSOR PROTEIN (APP) IS PROTECTIVE AGAINST IRON HOMESTASIS
DYSFUNCTION AFTER TREATMENT WITH ETHYL MALTOL**

by
Yuchen Kristine Sun

A thesis submitted to Johns Hopkins University in conformity with the requirements for
the degree of Master of Science

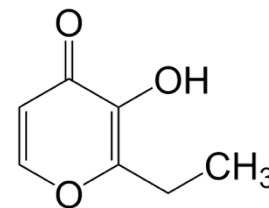
Baltimore, Maryland
April 2020

© 2020 Yuchen Kristine Sun

All rights reserved

Abstract

Ethyl Maltol (EM) is a flavoring compound commonly used in the food industry and has been reported to bind and mediate the transport of iron into cells (CDC, 2017). Since EM is highly lipophilic, it is hypothesized to easily pass through cellular plasmid membranes and blood brain barrier (BBB). Unwanted iron entry into the brain could be cytotoxic owing to the generation of reactive oxygen species. To protect against iron mediated cytotoxicity, several genes including amyloid precursor protein (APP) are involved in iron export. Several investigations have suggested a relationship between iron build-up and Alzheimer's disease (AD) (Shea et al., 2016). Risk attributable to genetics accounts for approximately 5% of AD cases (Shea et al., 2016). Accordingly, it is important to understand factors that increase the risk of AD such as lifestyle and environmental exposures.



Our hypothesis is that APP is protective against xenobiotics that disrupt iron homeostasis. Human neuroblastoma SH-SY5Y cell line was used because it expresses functions expressed by human neurons. We established the SH-SY5Y cell line overexpressing APP. The following assays were employed: MTT assay for cell viability; Calcein AM for labile iron; qRT-PCR and western blots for gene expression.

Cytotoxicity was observed in EM-treated cells for 72 hours at 0.3mM. Increases in p21 and 14-3-3 σ expression indicated the activation of a p53 response. The mechanism appears to involve disruption of iron homeostasis. Increases were detected in the expression of the iron transporter genes DMT1 and TfR1. Increases were also observed in labile iron which were confirmed in HEK293 using a reporter gene construct. Moreover, EM-mediated induction of DMT1 and TfR1 was attenuated in SH-SY5Y-APP cells. Our studies have the potential to help understand APP's function in neurons and its mechanisms in protecting against toxicity caused by iron dysfunction. Altered processing of APP might disrupt iron homeostasis resulting in neuronal death. Overall, our work provides novel insights regarding the etiology of AD and identifying factors that increase AD risks.

Primary Reader and Advisor: Dr. Joseph Bressler

Secondary Reader: Dr. Jonathan Coulter

Table of Contents

<i>Abstract</i>	<i>ii</i>
<i>Table of Contents</i>	<i>iii</i>
<i>List of Tables</i>	<i>iv</i>
<i>List of Figures</i>	<i>v</i>
1. Introduction	1
2. Materials and Methods	3
2.1 Cell culture	4
2.2 Establishing SH-SY5Y expressing amyloid precursor protein (APP).....	4
2.3 Transient transfections.....	5
2.4 The 4,5-dimethylthiazol-2-yl)-2,5-diphenyltetrazolium bromide (MTT) cell viability assay	5
2.5 RNA isolation and Real-Time PCR.....	6
2.6 Western blots.....	6
2.7 Intracellular iron measurement	7
2.8 Immunostaining for γ -H2AX.....	8
3. Results	8
3.1 EM is cytotoxic to SH-SY5Y cells and the overexpression of APP protects against EM-mediated toxicity.....	8
3.2 EM increases expression of the p53 regulated genes p21 and 14-3- σ and induced p21 was found in SH5Y-APP cells	9
3.3 EM induces the expression of divalent metal transporter 1 (DMT1) and transferrin receptor (TfR1) which are both attenuated in SH5Y-APP cells.....	10
3.4 EM increases labile iron in SH-SY5Y cells.....	11
3.5 EM causes decrease in Iron Responsive Proteins (IRPs) in HEK 293 cells	12
3.6 EM treatment increases DNA double strand breaks.....	13
3.7 Retinoic Acid Induced Differentiation SH-SY5Y cells.....	14
3.7.1 EM induces p21 gene expression.....	14
3.7.2 EM induces the expression of divalent metal transporter 1 (DMT1) and transferrin receptor (TfR1) in differentiated cells which are both attenuated in SH5Y-APP cells	15
4. Discussion	16
5. References	18
<i>Curriculum Vitae</i>	<i>21</i>

List of Tables

1. Table 1. Revers and forward primers used 6

List of Figures

1. Establishing an APP overexpressing SH-SY5Y cell line	4
2. EM dose response curve comparing naïve SY-SH5Y cells and SH-SY5Y APP cells	9
3. EM induces the expression of 14-3-3 σ and p21.....	9
4. EM increases expression of DMT1 and TfR1 in naïve and SH-SY5Y APP cells	11
5. Effect of EM on labile iron pool in SH-SY5Y cells	12
6. Effect of EM on iron responsive proteins (IRPs).....	13
7. EM increases the percentage of cells display γ -H2AX foci	15
8. Treatment with EM increases of p21 mRNA in differentiated cells	15
9. Effect of EM on DMT1 and TfR1 in differentiated SH-SY5Y cells	16

1. Introduction

Neurodegenerative diseases refer to disorders caused by the progressive death or loss of function of neurons (Fahn et al., 2011). Common neurodegenerative diseases include Parkinson's, Alzheimer's and Huntington's diseases. Alzheimer's disease (AD) currently affects 5 million people in the United States, with an approximate death rate of 55%, and this number is continuously increasing (CDC, 2017). The population over 65 years old is twice as likely to be diagnosed with AD, though symptoms and pathology likely begin years before diagnosis (Liu et al., 2018).

AD is characterized by memory loss at early stages, and dyslexia, directionality loss, and anxiety at later stages (Cheng et al., 2013). As the condition worsens, patients' mental activities, including cognitive behaviors and emotional reactions, and their regular body functions are affected (Ikonovic et al., 2011). Approximately 5% of AD cases are familial suggesting vast majority of cases involve environmental factors (Shea et al., 2016). Accordingly, it is important to learn about the environmental exposures and AD as well as other neurodegenerative diseases (Shea et al., 2016). The lack of cure for AD as well as the expansive and extensive care required for patients make it urgent to study this public health problem.

The pathogenesis of AD is primarily driven by extracellular deposition of β -amyloid and intracellular accumulation of tau protein (Agamanolis, 2016). β -amyloid ($A\beta$) is formed by the cleavage of a type I transmembrane protein — Amyloid Precursor Protein (APP) (Liu et al., 2018). During the amyloid degradation pathway of APP, peptides $A\beta_{40}$ and $A\beta_{42}$ are formed and can cause neurotoxicity and ultimately AD (Liu et al., 2018).

Disruption in iron homeostasis is also a possible factor involved in the development of AD. As an essential metal, iron is required in multiple cellular functions and participates in DNA, RNA and protein synthesis (Liu et al., 2018). Since the brain is an energy-demanding organ which requires iron for mitochondria to synthesis ATP, brain iron homeostasis is especially important. When iron homeostasis is disrupted, brain iron accumulation induces the formation of ferritin-associated plaques and can cause chronic neurological disorders including AD. This is in part because of the generation of reactive oxygen

species (ROS), causing lipid peroxidation and DNA damage. Multiple studies have found excess iron in AD patients' brains by both magnetic resonance imaging (MRI) data and biochemical measurements (Liu et al., 2018).

The homeostasis of iron in cells is tightly regulated by four major proteins. Transferrin receptor 1 (TfR1) and divalent metal transporter-1 (DMT1) regulate iron uptake, while ferroportin (FPN) regulates iron export and ferritin (Ft) regulates iron storage (Liu et al., 2018). The mRNAs of iron transporters have iron response elements (IRE) at the 3' untranslated regions and the mRNAs of FPN and ferritin have IREs at the 5' end. When cells are iron-deficient, iron-related proteins (IRPs) bind to the IRE resulting DMT1 and TfR mRNA stability and inhibition of FPN and ferritin translation. Consequently, more iron is brought into the cell. When iron levels are sufficient, ferritin and FPN protein are synthesized thereby decreasing levels of iron availability (Zhou et al., 2017).

In the intestine, non-heme iron is transported in the ferrous Fe^{2+} form through DMT1 (Liu et al., 2018). The absorbed iron can be stored in ferritin or exported out of the intestinal cell through FPN. In addition to the IRE, another layer of iron homeostasis is regulated at FPN. The polypeptide hepcidin binds to FPN and prevents the release of iron from cells (Silva et al., 2015). The unutilized Fe^{2+} will be oxidized to Fe^{3+} with the assistance of ferrous oxidase or ceruloplasmin and transported out of the cell through FPN1 located on the cell surface (Silva et al., 2015).

APP also has a role in regulating iron homeostasis in the brain. APP mRNA contains an IRE element in the 5'UTR that can bind to IRPs (Silva et al., 2015). An increase in the levels of APP protein was reported during iron influx due to increased translation of APP mRNA. (Cho et al., 2010). APP has been proposed to participate in iron homeostasis by stabilizing the iron exporter FPN. If cells lacked APP, it would be expected that higher levels of ferritin, and lower levels of TfR1 would be observed because less iron undergoes transport. Indeed, a previous study found higher levels of intracellular iron and ferritin, and lower levels of TfR1 in APP knockout mice (Wong et al., 2014). Additionally, it would be expected that the absence of APP would increase oxidative stress., considering that ferrous form mediates the generation of reactive oxygen/ nitrogen species (Tsatsanis et al., 2019).

Brain iron dysregulation can contribute to the development of AD not only through the generation of ROS but also the promotion of β -amyloid formation. In multiple studies, brain iron accumulation induced the aggregation and deposition of β -amyloid and neurofibrillary tangles formation through the interaction of iron with APP's IRE site (Silva et al., 2015). Iron has the ability to induce APP cleavage on the A β domain, causing the increased production of β -amyloid. The excess Fe³⁺ bound to β -amyloid is converted to Fe²⁺ through the redox activity and induce ROS, causing the cleavage of A β 42 into neurotoxic β -amyloid oligomers and development of AD (Lane et al., 2018).

Considering the involvement of iron homeostasis in AD, increased risk of AD might be due to exposure to xenobiotics that disrupt iron homeostasis. One such xenobiotic that has gained popularity is ethyl maltol (EM, C₇H₈O₃) because it is a common constituent in e-cigarettes. It is also widely used as an aromatic additive in food, beverages, pharmaceutical products, and health care products. The FDA classifies EM as “generally recognized as safe (GRAS)” if used at recommended levels, although the guidelines were based on very limited research (FDA, 2014). Recent studies show EM's possible role in facilitating uptake of metals and its ability to form a toxic EM-Fe complex (Li et al., 2017). Unwanted iron entry could be cytotoxic owing to the generation of reactive oxygen species (ROS).

Considering EM is highly lipophilic and volatile, EM could easily pass through the blood brain barrier and enter the brain, which raises the possibility that exposure to EM, and other xenobiotics that display interactions with iron, are risk factors for AD and other neurodegenerative diseases (Schoenborn et al., 2014, Li et al., 2017). The goal of my research is to determine whether EM mediates neuronal degeneration by disrupting iron homeostasis. My research is also examining the involvement of Alzheimer's Disease hallmark gene – Amyloid Precursor Protein (APP) in regulating iron. A disruption in APP processing could compromise the ability of the neuron to regulate iron homeostasis. The combination of the loss of APP, and exposure to chemicals such as EM that disrupt iron homeostasis, could lead to neuronal death and neurodegeneration.

1. Materials and Methods

2.1 Cell culture

The human neuroblastoma SH-SY5Y cell line was used to test our hypothesis. Cells were grown in Dulbecco Modified Eagle Medium (DMEM) high glucose with 10% fetal bovine serum (FBS). Cells were fed with fresh medium 3 times a week and passaged in 1:4 ratio with 0.25% trypsin when they reach about 80% confluency.

SH-SY5Y cells differentiate and form neurite and other phenotypes associated with neurons (Kovalevich et al., 2013). SH-SY5Y cells were differentiated with 10 μ M trans retinoic acid (RA) in media containing 2% FBS and antibiotics (Penn strep) at 1:100 dilution. Neurite outgrowth and the expression of neuronal markers were observed at 3 days after differentiation.

2.2 Establishing SH-SY5Y expressing amyloid precursor protein (APP)

SH-SY5Y cells were plated in 6-well plates at a density of 400,000 cells per well and transfected the following day with pEGFP-n1-APP (69924, Addgene) plasmid using the jetOPTIMUS transfection reagent from Polyplus-transfection. Transfected cells overexpressing APP were selected by adding 50 μ M of neomycin (G418) for 7 days. Resistant cells were grown and cryopreserved.

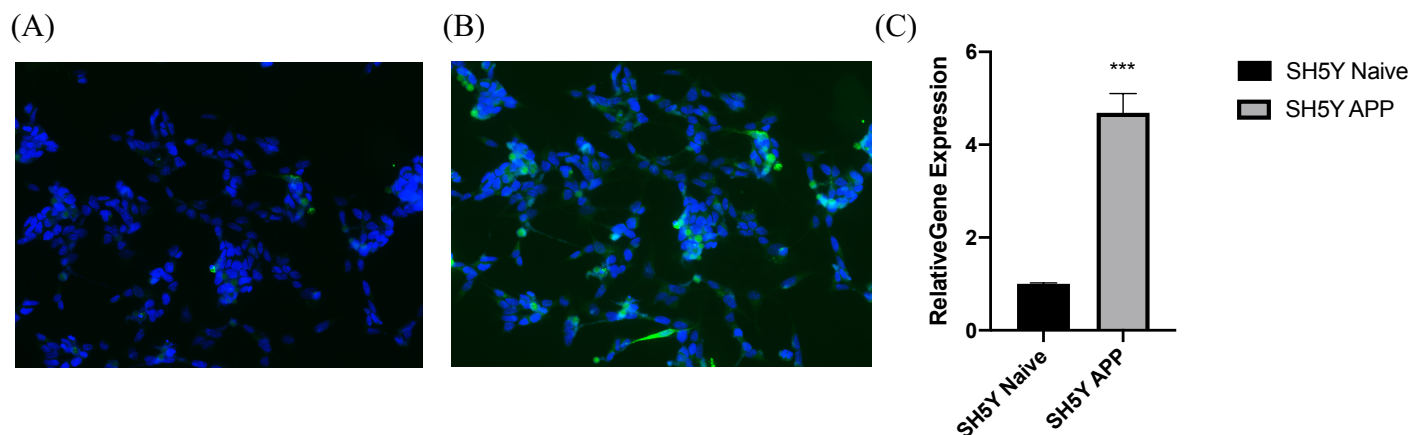


Figure 1. Establishing an APP overexpressing SH-SY5Y cell line. (A) Naïve SH-SY5Y cells (B) SH-SY5Y cells expressing high levels of APP (eGFP). (C) Relative expression of APP mRNA level comparing Naïve SH-SY5Y cells and selected SH-SY5Y APP cells. *Relative gene expression was quantified by normalizing to housekeeping gene RPLPO by Bio-Rad CFX manager software. Results are*

expressed as the mean \pm S.E.M. Unpaired T-test was performed to test the significance between two groups. F test was performed to compare variances. ***, $p < 0.01$ (One-sample t-test).

2.3 Transient transfections

HEK 293 cells were grown in DMEM with 10%FBS. Cells were plated in 6-well plates at a density of 400,000 cells per well and transfected with the IRE-containing plasmid pIRE-YIC (Clontech) the following day with jetOPTIMUS transfection reagent. Cells were transferred into 96-well plates and treated with ethyl maltol and deferoxamine 2 days after transfection.

2.4 The 4,5-dimethylthiazol-2-yl)-2,5-diphenyltetrazolium bromide (MTT) cell viability assay

The MTT assay is an indirect measurement of cellular respiration (Chacon et al., 1997). MTT is converted to MTT-formazan via mitochondrial dehydrogenase enzymes, resulting in a colorimetric change (Chacon et al., 1997). To conduct the assay, cells were plated in 96-well plates at a density of 40,000 cells per well and treated with EM at different concentrations at 24 hours after plating. MTT was made at a 12mM stock solution and added to the cells to achieve a 1.2mM final concentration. The cells were returned to the incubator, and at 2 hours after adding the MTT, media was aspirated from the wells and 200 μ L of dimethyl sulfoxide was added to each well to solubilize the MTT crystals. MTT-formazan absorbance was read at 540 nm wavelength on Molecular Devices SpectraMax M5 SoftMax Pro 7.0.3. Background absorbance was measured by adding 10% SDS to wells of untreated cells prior to adding MTT. Percent viability was computed by the following formula, where $\bar{X}_{experimental}$ refers to the average absorbance measurement of 6 biological replicates, \bar{X}_{SDS} refers to the average absorbance measurement of SDS background and $\bar{X}_{control}$ refers to the average absorbance measurement of medium control.

$$\frac{(\bar{X}_{experimental} - \bar{X}_{SDS})}{\bar{X}_{control}} * 100 = \% \text{ viability}$$

2.5 RNA isolation and Real-Time PCR

Total RNA was extracted from adherent SH-SY5Y cells with TRIzol Reagent. The phases were separated with chloroform and the RNA was precipitated with 100% isopropanol. The precipitate containing the total RNA was washed with 75% ethanol to remove impurities. RNA was resuspended in nuclease-free water and the concentration of RNA was quantified with NanoDrop. First-strand cDNA was synthesized using Oligo(dT)₁₂₋₁₈ (500 µg/mL), 10mM dNTP Mix, 5X first-strand Buffer, M-MLV RT reagent purchased from Invitrogen.

Levels of mRNA were quantified and analyzed using Bio-Rad CFX Manager software to compute the relative quantity (ΔCq) and normalized with housekeeping gene RPLPO to compute the normalized expression ($\Delta\Delta Cq$).

The primers sequences for amplification of the target genes can be found in table 1.

Table 1. Revers and forward primers used for RT-PCR.

Gene names	Forward 5' - 3'	Reverse 3' - 5'
RPLPO	GCAGCATCTACACTGAAG	CACTGGCAACATTGCGGAC
DMT1	GCCTTTATGGGTCCCGGATT	CAGCTTGTGACCCTGATTGC
APP	GGCCCTGGAGAACTACATCA	AATCACACGGAGGTGTGTCA
p21	TGGACCTGGAGACTCTCAGG	TCCAGGACTGCAGGCTTCCT
14-3- σ	GGCCATGGACATCAGCAAGAA	CGAAAGTGGTCTTGGCCAGAG
TfR1	ATACGTTCCCCGTTGTTGAGG	GGCGGAAACTGAGTATGGTTGA

2.6 Western blots

SH-SY5Y cells and SH-SY5Y APP cells were plated at 2,000,000 cells per 10 cm² plate and treated at 24 hours after plating. To harvest protein, cells were collected by scraping into PBS, pelleted, and protein was extracted with RIPA lysis buffer containing protease inhibitor and phosphatase inhibitor. Lysates were sonicated and placed on ice for 30 minutes. Soluble protein was isolated by centrifuging

lysates at 15,000g for 10 minutes and then harvesting the supernatant. Protein concentration was measured using the Bradford assay with Molecular Devices SpectraMax M5 SoftMax Pro 7.0.3.

SDS-PAGE was performed on 4-20% gels subjected to 200 and 400 mA for 40 minutes. Protein was transferred to a nitrocellulose membrane at 200V, 400 mA for 1 hour. The nitrocellulose membrane was incubated with 1X PBS+ 1% Casein Blocker (Bio-Rad) for 1 hour to prevent non-specific binding. The nitrocellulose membrane was incubated with primary antibodies Transferrin receptor 1 (CD71, D7G9X XP Rabbit mAb from Cell Signaling) at 1:1000 and p21 (Waf1/Cip1 (12D1) Rabbit mAb from Cell Signaling) at 1:1000 overnight at 4 °C. After washing, the secondary antibody IRDye® 800CW Goat anti-Rabbit IgG (Li-cor) was added for an hour at room temperature. After washing, images were taken with Li-cor Odyssey. Band density was analyzed with Image Studio. Levels of p21 and TfR1 are expressed by normalizing to β -actin (Sigma-Aldrich, A1978).

2.7 Intracellular iron measurement

The cellular labile iron pool (LIP) consists of iron not bound to protein and can trigger the generation of reactive oxygen species (ROS). The fluorescent dye Calcein AM is used to measure the LIP because it binds to labile iron resulting in quenching. SH-SY5Y cells were plated in 24-well plates at a concentration of 50,000 cells per well, and treated with Ethyl Maltol or deferoxamine at one day after plating. After a 24-hour treatment, medium was aspirated and Calcein AM (RnD Systems, 4892-010-K) was added to cells at a final concentration of 4 μ M. Cells were trypsinized after a 15-minute incubation with calcein and transferred into 96-well Costar Black Walled plate at 30,000 cells per well. Level of fluorescence was read at 490 nm excitation and 520 nm emission wavelength on Molecular Devices SpectraMax M5 SoftMax Pro 7.0.3.

2.8 Immunostaining for γ -H2AX

γ -H2AX foci indicate sites where DNA double strand breaks are being repaired. SH-SY5Y cells were plated on poly-L-lysine (PDL)-coated cover slips at 50,000 cells per well in 24-well plates. SH-SY5Y cells were treated with Ethyl Maltol for 36 hours. Positive control was accessed with treatment with 3 μ M etoposide for 2 hours. SH-SY5Y cells were fixed with 4% PFA for 20 minutes and permeabilized with 0.2% Triton-X-100 for 10 minutes. Cells were incubated with 1% PBS-BSA to prevent nonspecific binding of antibodies. Antibody against γ -H2AX (Ser139) primary antibody (mouse monoclonal, clone JBW301, EMD Millipore; #05-636) (2 μ g/mL) was added overnight at 4 °C. After cells were washed with PBS, fluorescent labeled Goat anti-Mouse IgG Secondary Antibody was added for 1 hour at room temperature. After washing with PBS, coverslips were mounted onto slides with 4',6-diamidino-2-phenylindole (DAPI) to stain nuclei and anti-fade reagent. Percentage of cells display foci was computing by dividing the number of cells with 5 foci or more by the total number of cells and multiplying by 100.

2. Results

3.1 EM is cytotoxic to SH-SY5Y cells and the overexpression of APP protects against EM-mediated toxicity

Cell viability should be compromised after exposing cells to chemicals that disrupt iron homeostasis. Indeed, approximately a 50% decrease in viability was observed in SH-SY5Y after a 72-hour treatment with 1 mM EM (Fig. 2). In contrast, an approximately 25% decrease in viability was observed in the SH-SY5Y overexpressing APP at 1mM EM.

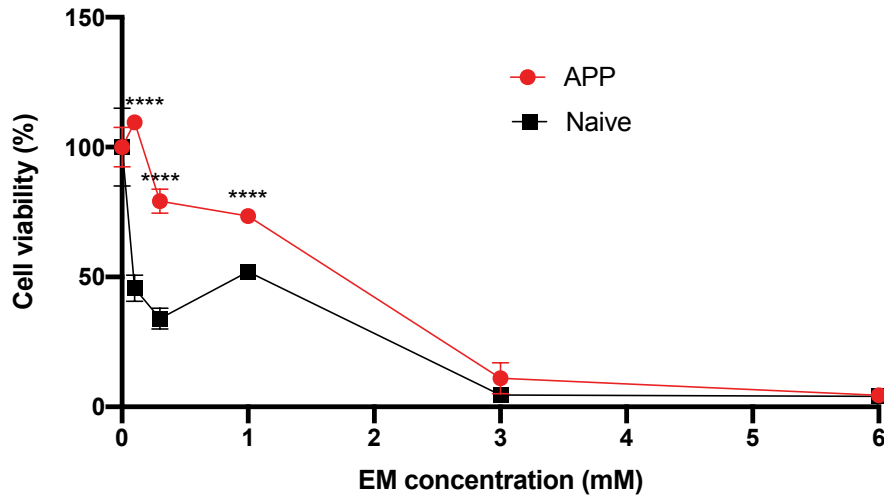
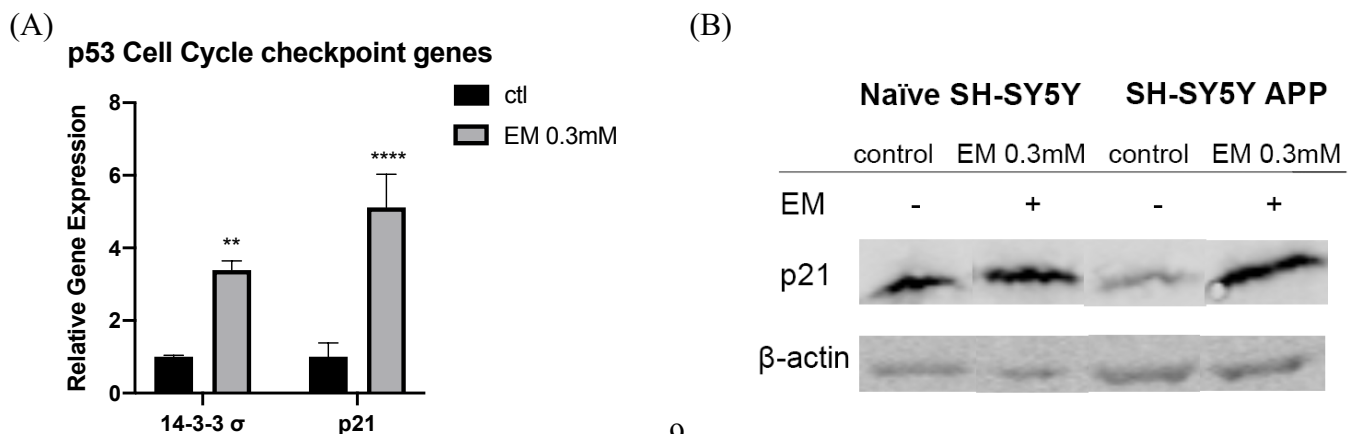


Figure 2: EM dose response curve comparing naïve SH-SY5Y cells and SH-SY5Y cells over expressing APP. A dose response curve was generated with Prism 8 in the method of one-way ANOVA and a Tukeys's HSD was performed to validate the normality of the data. Each value is derived from 6 replicates \pm S.E.M. ****, $p < 0.0001$.

3.2 EM increases expression of the p53 regulated genes p21 and 14-3- σ and induced p21 was found in SH5Y-APP cells

The p53 pathway is activated when cells undergo stress responses such as hypoxia and DNA damage resulting in the inhibition of the cell cycle. Levels of the cell cycle checkpoint genes 14-3-3 σ and p21 mRNA increased by 2-fold and 3-fold, respectively, when treated with 0.3mM EM for 72 hours (Fig.3A). About 4-fold induction of p21 relative protein levels was found in SH-SY5Y APP cells while less than 1-fold induction was found in naïve SH-SY5Y cells (Fig. 3B, C).



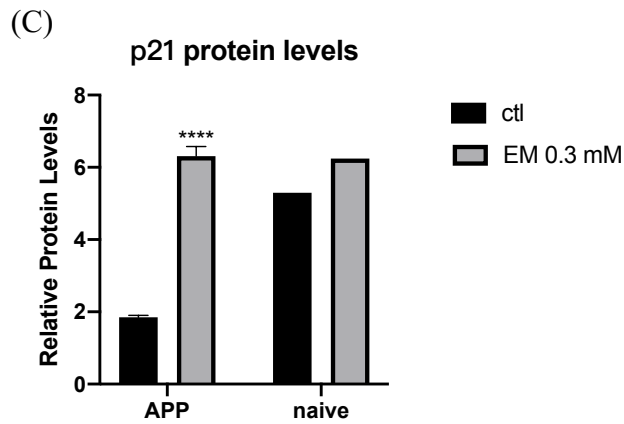


Figure 3: **EM induces the expression of 14-3-3 σ and p21.** (A) *Relative gene expression was quantified by measuring levels of mRNA and normalizing to RPLPO by Bio-Rad CFX manager software.* (B) *Western blot analysis of p21 and β -actin.* (C) *Relative protein levels were analysed with Image Studio and normalized to β -actin. **, $p < 0.05$. ****, $p < 0.0001$ (ANOVA, Tukey posthoc test)*

3.3 EM induces the expression of divalent metal transporter 1 (DMT1) and transferrin receptor (TfR1) which are both attenuated in SH5Y-APP cells

Given that EM binds iron and is also highly membrane permeable, the possibility was investigated that EM decreases viability by disrupting intracellular iron homeostasis. Greater than a 20-fold induction in DMT1 mRNA was observed in SH-SY5Y cells treated with 0.3mM EM for 72 hours compared to the control group (Fig.4A). In contrast, the induction of DMT1 was 5-fold in the APP expressing SH-SY5Y cells. EM also induced TfR1 mRNA expression in SH-SY5Y cells treated with 0.3mM EM for 72 hours (Fig.4B). A 1.5- fold increase was observed in TfR after treatment with EM for 72 hours at 0.3mM (Fig.4C, D). Interestingly, the TfR1 mRNA was elevated in APP expressing cells without EM treatment and no further induction was observed with EM. A 1.5- fold induction was observed in TfR protein after treatment with EM for 72 hours at 0.3mM (Fig.4C, D).

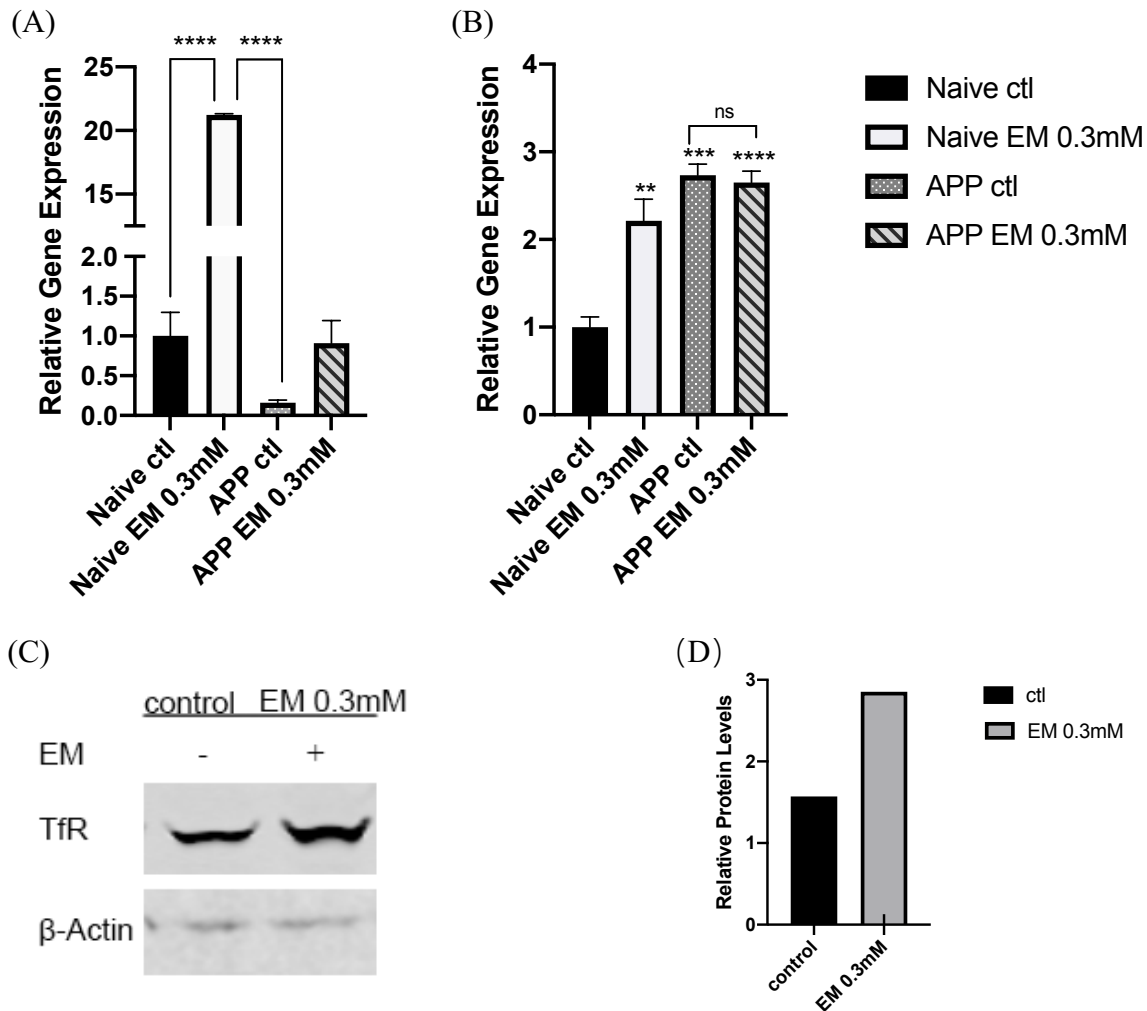


Figure 4: EM increases expression of DMT1 and TfR1 in naïve and less in APP overexpressing SH-SY5Y cells. (A) DMT1 and (B) TfR1 mRNA levels are expressed normalized to RPLPO using Bio-Rad CFX manager software. Results are expressed as the mean \pm S.E.M.. (C) Western blot analysis of TfR. (D) Relative protein levels were analyzed with Image Studio and normalized to β -actin. **, $p < 0.05$. ***, $p < 0.01$. ****, $p < 0.0001$. ns, not significant. (ANOVA, Tukey posthoc test)

3.4 EM increases labile iron in SH-SY5Y cells

The iron in the cell not bound to protein is referred to as the labile iron pool (LIP) and is analysed with the fluorescent dye calcein. Fluorescence quenching indicates increases in the LIP. Significant decreases were observed in fluorescence in cells with 24-hour EM treatment at 0.3 mM and 0.1 mM

(Fig.5). Previous experiments have confirmed that no effect of EM on cell viability at 24 hours, indicating the decrease in calcein fluorescence is due to increase in LIP not cell death (data not shown here). Similarly, deferoxamine (DFE), a known iron chelator, was also found to increase LIP resulting in calcein fluorescence reduction (Fig.5).

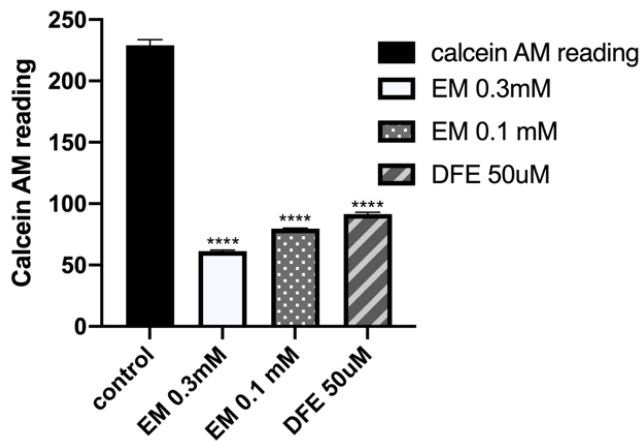


Figure 5: **Effect of EM on labile iron pool in SH-SY5Y cells.** *Calcein AM reading was taken at 490 nm excitation and 520nm emission. ****, $p < 0.0001$ (ANOVA, Tukey posthoc test)*

3.5 EM causes decrease in Iron Responsive Proteins (IRPs) in HEK 293 cells

The bicistronic reporter construct was used to measure levels of IRP. The reporter genes are Yellow Fluorescence Protein (YFP) and Cyan Fluorescence Protein (CFP). CFP is constitutively expressed whereas YFP is regulated by an intracellular iron element located at the 5' UTR. IRP binds to the 5'- of the mRNA resulting in a decrease in YFP mRNA translation (Fig. 6A). The assay was conducted in HEK293 cell line because of the better transfection efficiency. Treatment with EM at all concentrations for 24 hours caused significant decrease in YFP/CFP ratio (Fig. 6B). This means that IRP level was greatly enhanced with EM treatment even at 0.3mM.

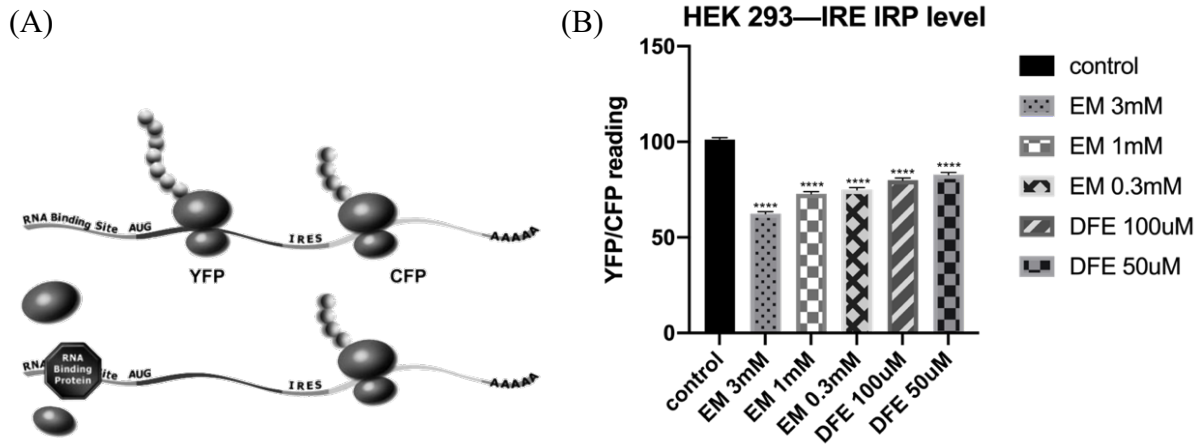


Figure 6. **Effect of EM on iron responsive proteins (IRPs).** (A) Schematic representation of the bicistronic reporter gene constructs. *The RNA binding site is an IRE that will interact with the RNA binding protein iron response protein (IRP) resulting in less translation.* (B) Assessment of IRP–IRE interaction in HEK 293 cells after transient transfection of the IRE-containing bicistronic reporter gene. *Deferoxamine (DFE), a known iron chelator, was used as the positive control. ****, $p < 0.0001$ (ANOVA, Tukey posthoc test).*

3.6 EM treatment increases DNA double strand breaks

Given that excess amount of intracellular iron can induce DNA damage, the effect of EM was determined on DNA integrity by measuring the percentage of cells with γ -H2AX foci. Foci were not observed in untreated cells (Fig.7A). EM at 0.3mM and 1mM increased foci formation (Fig. 7C, D). Topoisomerase II Inhibitor etoposide was used as a positive control. As expected, an increase in the percentage of cells forming foci was observed following etoposide exposure (Fig.7B).

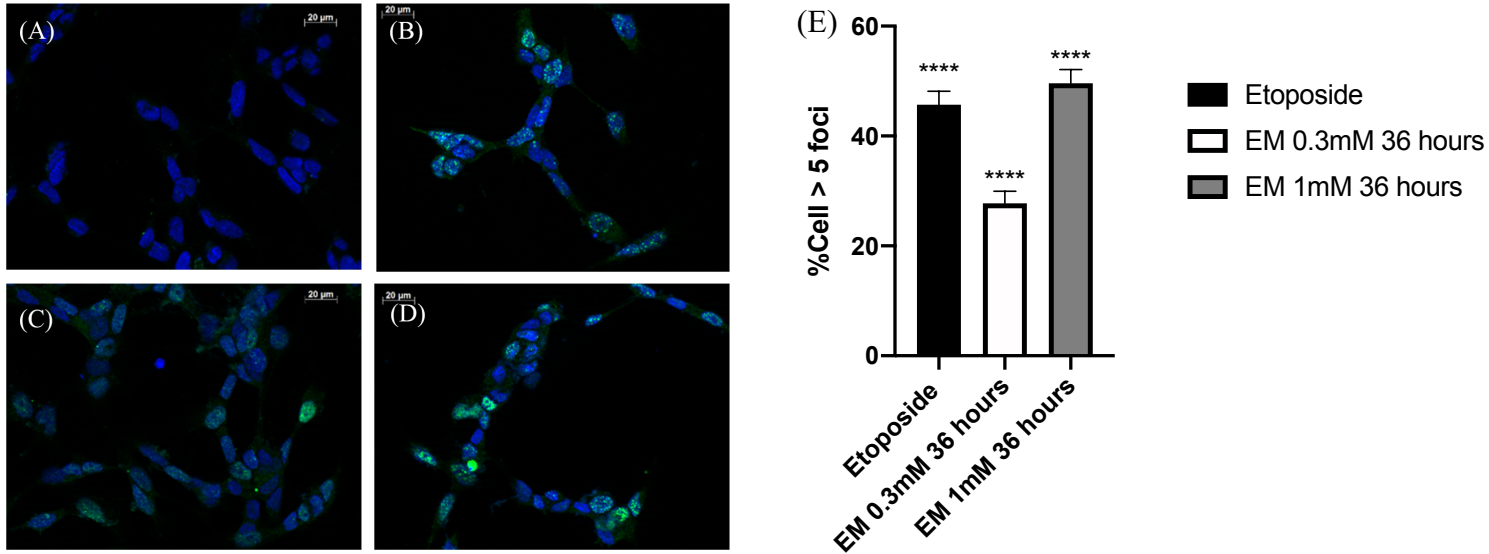


Figure 7. **EM increases the percentage of cells display γ -H2AX foci.** (A) control (B) etoposide (C) EM 0.3mM 36 hours (D) EM 1mM 36 hours quantification of number of foci per 100 DAPI positive cells.

Results are expressed as the mean of 6 technical replicates \pm S.E.M and variation was analyzed with one-way ANOVA. ****, $p < 0.0001$ (ANOVA, Tukey posthoc test).

3.7 Retinoic Acid Induced Differentiation SH-SY5Y cells

The next series of experiments focused on the effects of EM on differentiated SH-SY5Y cells. RA and other neurotrophic factors have been shown to increase neurite outgrowth and other markers of differentiated neurons in SH-SY5Y cells.

3.7.1 EM induces p21 gene expression.

In addition to induction of p21 levels in naïve SH-SY5Y cells after EM treatment, a 2-fold increase in p21 level was seen again in differentiated SH-SY5Y cells (Fig.8).

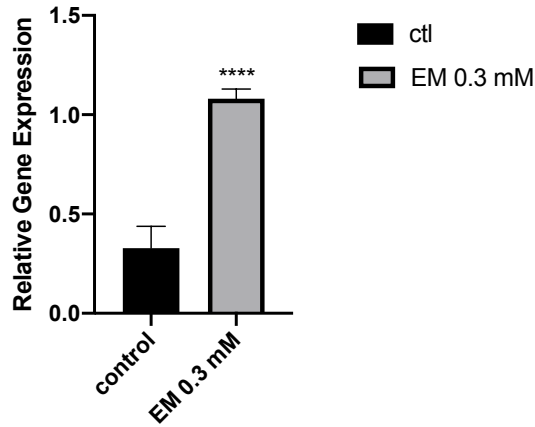


Figure 8. **Treatment with EM increases of p21 mRNA.** EM increases the expression of p21 in RA-induced SH-SY5Y cells. *Relative gene expression was quantified by normalizing to RPLPO by Bio-Rad CFX manager software. ****, $p < 0.0001$ (ANOVA, Tukey posthoc test).*

3.7.2 EM induces the expression of divalent metal transporter 1 (DMT1) and transferrin receptor (TfR1) in differentiated cells which are both attenuated in SH5Y-APP cells

EM also affects iron homeostasis in differentiated cells. Greater than a 10-fold induction in DMT1 mRNA was observed in differentiated SH-SY5Y cells treated with 1mM EM for 72 hours compared to the control group (Fig.9A). EM also induced TfR1 mRNA expression in SH-SY5Y cells treated with 1mM EM for 72 hours by more than 5-fold and more than 10-fold at 0.3mM (Fig.9A). In contrast, DMT1 mRNA level was elevated in differentiated APP expressing SH-SY5Y cells and no further change was observed with EM treatment (Fig.9B). TfR1 mRNA was also elevated in differentiated APP expressing cells without EM treatment and only about 5-fold elevation of TfR mRNA level was found after treatment with EM for 72 hours at 0.3mM (Fig.9B).

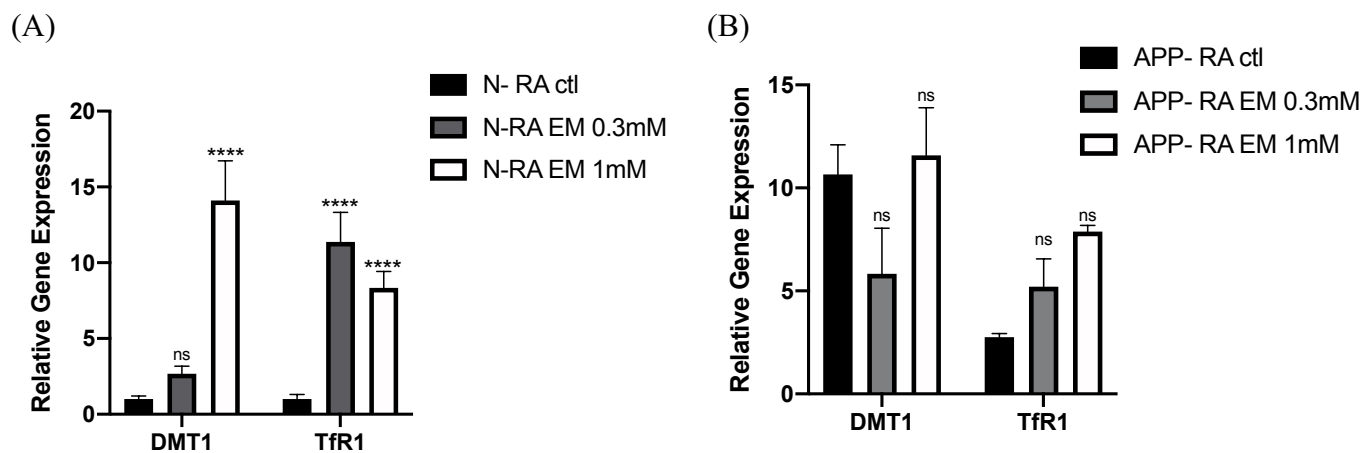


Figure 9. **Effect of EM on DMT1 and TfR1 in differentiated SH-SY5Y cells.** Treatment with EM increases DMT1 and TfR1 mRNA expression in differentiated SH-SY5Y cells, which is attenuated in selected concentrations in SH-SY5Y cells overexpression of APP. (A,B) Samples were amplified in duplicates and relative gene expression was analyzed using Bio-Rad CFX manager software and normalized to RPLPO. Results are expressed as the mean \pm S.E.M. Two-way ANOVA and multiple comparison were performed to generate P values between groups. ****, $p < 0.0001$. ns, not significant.

3. Discussion

Our study is the first report that EM decreases cell viability in a neuron model. Viability was not detected after cells were exposed to EM at 1 mM for 48 hrs. The decrease in viability was likely attributed to DNA damage. An increase was observed in the percentage of cells displaying γ -H2AX foci. The foci represent sites of DNA deletions that are undergoing repair. γ -H2AX is the product of H2AX phosphorylation by ATM and ATM is the master regulator of the DNA damage response (Celeste et al., 2003). The response has three branches including DNA repair, inhibiting the cell cycle, and apoptosis if the cell cannot sufficient repair the DNA. The latter two branches are induced through the activation of p53 (Celeste et al., 2003). Cell cycle inhibition is mediated by p53-mediated transcription of several genes including 14-3-3 σ and p21. Considering we observed increased expression of 14-3-3 σ and p21, it appears that the EM is activating the p53 pathway.

We suggest that EM decreases viability by disrupting iron homeostasis. Dramatic increases were observed in DMT1 and TfR1, which are membrane proteins that mediate iron uptake. The mRNA of both genes has an IRE at the 3'UTR that binds to an IRP when iron levels are low. The increases in mRNA stability results in increases in iron transport. EM was found to increase binding of IRP to the IRE in the IRP reporter assay. We suggest that EM freely enters cells because it is a highly lipophilic compound and binds to the iron inside the cell. Because the intracellular iron is not available, IRP binds to IRE resulting in DMT1 and TfR1 mRNA stability. Increases in DMT1 and TfR would result in increases in iron uptake. Nie et al also found that deferoxamine induces IRP levels in the same reporter assay (Nie et al., 2006). It is interesting that EM increases IRP binding to IRE and also increases the labile iron pool (LIP). Cells with sufficient levels of iron would not need more iron transport. Indeed, deferoxamine was shown to decrease the LIP. However, in a study on nitric oxide, investigator reported increases in both IRP and the labile iron pool. We suggest that different small molecular weight compounds will differentially affect iron homeostasis. The differences could be due to the permeability of the compound across the plasma, membrane, the half-life the compound inside the cells, and the mechanism in which the compound affects iron homeostasis.

Our data suggest a mechanism by which APP protects the cells against EM induced toxicity. A higher concentration of EM was needed to kill SH-SY5Y cells overexpressing APP and less induction in DMT1 and TfR1 mRNA level was observed. These findings indicate APP's potential ability to protect the cells from overload of iron. APP was shown to be involved in facilitating ferroportin (FPN1)-dependent toxic iron export at the plasma membrane of neurons, microglia, and astrocytes and can promote iron release as well as lower the LIP (Duce et al., 2010). In addition, an IRE was found at the 5' untranslated region of APP, which assists in down-regulating iron overload (Rogers et al., 2002). These findings help explain APP's role in assisting iron export and therefore protects neurons from iron-induced cytotoxicity.

In conclusion, we have found that EM induces cellular toxicity through the disruption of iron homeostasis, p53 pathways and associated DNA damage. We also found that the expression of APP

protects cells most likely by decreasing iron uptake and increasing iron export. While EM is still a widely used flavoring additive in many aspects, we are suggesting a re-evaluation of this chemical.

4. References

Bajbouj, K., Shafarin, J., & Hamad, M. (2018). High-Dose Deferoxamine Treatment Disrupts Intracellular Iron Homeostasis, Reduces Growth, and Induces Apoptosis in Metastatic and Nonmetastatic Breast Cancer Cell Lines. *Technology in Cancer Research & Treatment*, 17, 153303381876447. doi: 10.1177/1533033818764470

Barrand, M. A., Callingham, B. A., & Hider, R. C. (1987). Effects of the pyrones, maltol and ethyl maltol, on iron absorption from the rat small intestine. *Journal of Pharmacy and Pharmacology*, 39(3), 203–211. doi: 10.1111/j.2042-7158.1987.tb06249.x

Celeste, A., Difilippantonio, S., Difilippantonio, M. J., Fernandez-Capetillo, O., Pilch, D. R., Sedelnikova, O. A., ... Nussenzweig, A. (2003). H2AX Haploinsufficiency Modifies Genomic Stability and Tumor Susceptibility. *Cell*, 114(3), 371–383. doi: 10.1016/s0092-8674(03)00567-1

Celeste, A., Fernandez-Capetillo, O., Kruhlak, M. J., Pilch, D. R., Staudt, D. W., Lee, A., ... Nussenzweig, A. (2003). Histone H2AX phosphorylation is dispensable for the initial recognition of DNA breaks. *Nature Cell Biology*, 5(7), 675–679. doi: 10.1038/ncb1004

Centers for Disease Control and Prevention. (2017). CDC features - Alzheimer's Disease. Retrieved November 6, 2019, from <https://www.cdc.gov/features/alzheimers-disease-deaths/index.html>.

CHACON, E., ACOSTA, D., & LEMASTERS, J. J. (1997). Primary Cultures of Cardiac Myocytes as In Vitro Models for Pharmacological and Toxicological Assessments. *In Vitro Methods in Pharmaceutical Research*, 209–223. <https://doi.org/10.1016/B978-012163390-5.50010-7>

Dimitri, P., Agamanolis, M. D. (2016). Degenerative Diseases: Alzheimer's Disease. *Neuropathology, An illustrated interactive course for medical students and residents*. Chapter 9.

Duce, J. A., Tsatsanis, A., Cater, M. A., James, S. A., Robb, E., Wikhe, K., ... Bush, A. I. (2010). Iron-Export Ferroxidase Activity of β -Amyloid Precursor Protein Is Inhibited by Zinc in Alzheimers Disease. *Cell*, 142(6), 857–867. doi: 10.1016/j.cell.2010.08.014

Fahn, S., & Jankovic, J. (2011). *Principles and Practice of Movement Disorders* (2nd ed.). doi: <https://doi.org/10.1016/B978-1-4377-2369-4.00012-3>

Kovalevich, J., & Langford, D. (2013). Considerations for the Use of SH-SY5Y Neuroblastoma Cells in Neurobiology. *Neuronal Cell Culture Methods in Molecular Biology*, 9–21. doi: 10.1007/978-1-62703-640-5_2

Lane, D. J. R., Ayton, S., and Bush, A. I. (2018). Iron and Alzheimer's disease: an update on emerging mechanisms. *J. Alzheimers Dis.* 64, S379–S395. doi: 10.3233/JAD-179944

Li, Z., Lu, J., Wu, C., Pang, Q., Zhu, Z., Nan, R., ... Chen, J. (2017). Toxicity Studies of Ethyl Maltol and Iron Complexes in Mice. *BioMed Research International*, 2017, 1–9. doi: 10.1155/2017/2640619

Liu, J.-L., Fan, Y.-G., Yang, Z.-S., Wang, Z.-Y., & Guo, C. (2018). Iron and Alzheimer's Disease: From Pathogenesis to Therapeutic Implications. *Frontiers in Neuroscience*, 12. doi: 10.3389/fnins.2018.00632

Maden, M. (2001). Role and distribution of retinoic acid during CNS development. *International Review of Cytology*, 1–77. doi: 10.1016/s0074-7696(01)09010-6

Nie, M., & Htun, H. (2006). Different modes and potencies of translational repression by sequence-specific RNA–protein interaction at the 5'-UTR. *Nucleic Acids Research*, 34(19), 5528–5540. doi: 10.1093/nar/gkl584

Rogers, J. T., Venkataramani, V., Washburn, C., Liu, Y., Tummala, V., Jiang, H., ... Cahill, C. M. (2016). A role for amyloid precursor protein translation to restore iron homeostasis and ameliorate lead (Pb) neurotoxicity. *Journal of Neurochemistry*, 138(3), 479–494. doi: 10.1111/jnc.13671

Shea, Y.-F., Chu, L.-W., Chan, A. O.-K., Ha, J., Li, Y., & Song, Y.-qiang. (2016). A systematic review of familial Alzheimer's disease: Differences in presentation of clinical features among three

mutated genes and potential ethnic differences. *Journal of the Formosan Medical Association*, 115(2). doi: <https://doi.org/10.1016/j.jfma.2015.08.004>

Silva, B., & Faustino, P. (2015). An overview of molecular basis of iron metabolism regulation and the associated pathologies. *Biochimica Et Biophysica Acta (BBA) - Molecular Basis of Disease*, 1852(7), 1347–1359. doi: <https://doi.org/10.1016/j.bbadis.2015.03.011>

Torti, S. V., & Torti, F. M. (2013). Iron and cancer: more ore to be mined. *Nature Reviews Cancer*, 13(5), 342–355. doi: 10.1038/nrc3495

Wu, Y., Li, X., Xie, W., Jankovic, J., Le, W., & Pan, T. (2010). Neuroprotection of deferoxamine on rotenone-induced injury via accumulation of HIF-1 α and induction of autophagy in SH-SY5Y cells. *Neurochemistry International*, 57(3), 198–205. doi: 10.1016/j.neuint.2010.05.008

Curriculum Vitae

Surname, first name: Sun, Yuchen (Kristine)

Address: 929 N. Wolfe St. Apt 2009 B, Baltimore, MD, 21205

Telephone: (443)500-4989

Date of birth: 11/22/1995

Country of birth: China

Email: ysun95@jhmi.edu/ sunyuchen22@hotmail.com

EDUCATION

Johns Hopkins University, Baltimore, MD

September 2018 - Present

- Master of Science - Environmental Health Engineering

expected graduation date 5/21/2020

University of Washington, Seattle, WA

September 2014 – August 2017

- Bachelor of Arts - Biochemistry

Selected coursework: Statistical Machine Learning— Methods, Theory, and Applications; Statistics for Laboratory Scientists I & II; Statistical Reasoning in Public Health I & II; Public Health Toxicology; Molecular Toxicology; Risk Assessments (Certified in Risk Science and Public Policy); Public Health Epidemiology I & II; Molecular Epidemiology

RESEARCH EXPERIENCE

Hugo W. Moser Research Institute at Kennedy Krieger

Johns Hopkins University, Baltimore

Graduate Researcher PI: Dr. Joseph Bressler

Winter 2018 – Present

- Disruption of iron homeostasis in neurological function
- Effect and mechanism of Amyloid Precursor Protein (APP) in protecting iron-induced neural damage

Laboratory for Computational Sensing and Robotics (LCSR)

Johns Hopkins University, Baltimore

Developer PI: Dr. Gregory Chirikjia

Fall 2019 – Present

- “Hopkins Women Soccer Dataset” development
- Using deep neural network to recognize human joints and human actions

SYAU Biochar Engineering Technology Research Laboratory

Shenyang Agricultural University, China

Lab Assistant PI: Dr. Jun Meng

Summer 2017 – Summer 2018

- Effects and applications of biochar on microbial communities
- Data analyses on soil toxin reduction rates using R

Larson Research Group (Brenowitz Lab)

University of Washington, Seattle

Undergraduate Researcher PI: Dr. Tracy Larson, Eliot Brenowitz

Winter 2015 – Summer

2017

- Genetics of neural organization and behavior in white-crowned sparrow
- Spectral features analyses and cross correlation of data on neuronal birth, incorporation, and death during the rapid growth of HVC

Parichy Laboratory

University of Washington, Seattle

Undergraduate Researcher PI: Dr. David Parichy

Spring 2015 – Spring 2016

- Roles for thyroid hormone in specifying cell fate and morphogenesis
- Breeding, injecting and screening observed under epifluorescence stereomicroscopes

INTERN & WORKING EXPERIENCE

McMahon Front Desk

University of Washington, Seattle

Desk Service Representative

Summer 2016 – Summer 2017

- Customer service, student service and financial analyses
- Helped support academic study and developed strong communication skills

MEMBERSHIP & LEADERSHIP EXPERIENCE

Society of Toxicology (SOT) – Student Member

2019 – present

YMCA Phinney Ridge – Volunteer Mentor

2016 – 2017

UW Dream Project – Student Mentor

2015 – 2017

Paws Cat City – Volunteer Veterinary Assistant

2015 – 2016

Husky Help Organization – Public Relationship Manager

2014 – 2015

Foundation for International Understanding Through Students (FIUTS) — Facilitator 2014 – 2015

SKILLS

- Histology: Cyrosectioning, Nissl staining, Microtome sectioning & Float mounting, Vibrotome and freezing, cell proliferation (Brd-U), Immunohistochemistry
- Biochemical: Immunodotblotting, Western Blot, Gel Electrophoresis, Mass Spectrometry
- Microscopy: Confocal, Immunofluorescent, bright field, imaging with Zeiss, Image J platforms, optical sectioning with Zeiss apotome
- Cell based assays: MTT assay, Annexin V, JC-1 fluorescent
- Molecular: quantitative RT-PCR; transgenic screening
- Statistical Programs: R, Excel, Prism
- Transient transfection, colony selection, minipreps/ plasmid DNA isolation
- Song Analysis: Song Sorting & Cutting (Syrinx), Spectral Features (Raven), Cross Correlation, Excel
- Basic Animal Care & Husbandry (fish, bird): Food preparation, Feeding, Enrichment
- Tissue culture maintenance
- Behavior analyses (Tracker), Sexing & breeding (zebra fish)
- Risk assessment, communication and management
- Wildlife Photographer
- Language: Mandarin (Native Speaker), English (fluent), French (Rudimentary)